Molecular responses of alveolar epithelial A549 cells to chronic exposure to titanium dioxide nanoparticles: A proteomic view.

Lucie Armand, Mathilde Biola-Clier, Laure Bobyk, Véronique Collin-Faure, Hélène Diemer, Jean Marc Strub, Sarah Cianférani, Alain van Dorsselaer, Nathalie Herlin-Boime, Thierry Rabilloud, et al.

This document is an author version of the manuscript that has been published in Journal of Proteomics (2016) 134 : 164-173, under the doi: 10.1016/j.jprot.2015.08.006

Molecular responses of alveolar epithelial A549 cells to chronic exposure to titanium dioxide nanoparticles: a proteomic view.

Armand Lucie[1,2], Biola-Clier Mathilde[1,2], Bobyk Laure [1,2], Collin-Faure Véronique[3], Diemer Hélène[4], Strub Jean-Marc[4], Cianferani Sarah[4], Van Dorsselaer Alain[4], Herlin-Boime Nathalie[5], Rabilloud Thierry[6,§] and Carriere Marie[1,2,§]

[1]Université Grenoble-Alpes, INAC-LCIB, Laboratoire Lésions des Acides Nucléiques, 17 rue des Martyrs, F-38000 Grenoble, France.

[2]CEA, INAC-SCIB, Laboratoire Lésions des Acides Nucléiques, 17 rue des Martyrs, F-38054 Grenoble, France.

[3]CEA Grenoble, iRTSV/CBM, Laboratory of Chemistry and Biology of Metals, Grenoble, France

[4]Laboratoire de Spectrométrie de Masse BioOrganique (LSMBO), Université de Strasbourg, IPHC, 25 rue Becquerel 67087 Strasbourg, France. CNRS, UMR7178, 67037 Strasbourg, France.

[5]UMR3685 CEA-CNRS, NIMBE, LEDNA, CEA Saclay, F-91191 Gif sur Yvette, France.

[6]CNRS UMR 5249, Laboratory of Chemistry and Biology of Metals, Grenoble, France

[§]Corresponding authors: Marie Carriere, CEA Grenoble, LAN, Bât C5, Pce 632, 38054 Grenoble Cedex 9, France. Phone: +33 4 38 78 03 28, fax: +33 4 38 78 50 90. marie.carriere@cea.fr ; Thierry Rabilloud, CNRS-LCBM ProMD team, CEA Grenoble, Bât C3, 38054 Grenoble Cedex 9, France. Phone: +33 4 38 78 32 12. thierry.rabilloud@cnrs.fr, fax: +33 4 38 78 44 99.

Abstract

Although the biological effects of titanium dioxide nanoparticles (TiO_2-NPs) have been studied for more than two decades, the mechanisms governing their toxicity are still unclear. We applied 2D-gel proteomics analysis on A549 epithelial alveolar cells chronically exposed for 2 months to 2.5 or 50 µg/mL of deeply characterized TiO_2-NPs, in order to obtain comprehensive molecular responses that may reflect functional outcomes. We show that exposure to TiO_2-NPs impacts the abundance of 30 protein species, corresponding to 22 gene products. These proteins are involved in glucose metabolism, trafficking, gene expression, mitochondrial function, proteasome activity and DNA damage response. Besides, our results suggest that p53 pathway is activated, slowing down cell cycle progression and reducing cell proliferation rate. Moreover, we report increased content of chaperones-related proteins, which suggests homeostasis re-establishment. Finally, our results highlight that chronic exposure to TiO_2-NPs affects the same cellular functions as acute exposure to TiO_2-NPs, although lower exposure concentrations and longer exposure times induce more intense cellular response.

Introduction

Titanium dioxide microparticles (TiO_2) have been used for over a century as a pigment in paints and cements. Since the use of TiO_2 nanoparticles (TiO_2-NPs) is continuously increasing, for instance as a catalyst or in self-cleaning surfaces, the production of TiO_2-NPs is predicted to soon overtake that of TiO_2 microparticles [1]. Original properties of nanoscale particles implies that they may cause different types of adverse effects [2]. So far, the mechanisms governing TiO_2-NP toxicity are not totally understood. Studies related to the toxicity of particulate matter have mainly focused on the lung, as it is the most problematic exposure route [2]. They were historically based on results obtained by the community working on the impact of environmental pollution with ultrafine particles. On this target, ultrafine particles (less than 2.5 µm in diameter) are known to induce oxidative stress, inflammation, genotoxicity, apoptosis, cytotoxicity and eventually cancer [3]. Therefore *in vitro* and *in vivo* studies related to TiO_2-NP toxicity have focused on the same endpoints, and particularly oxidative stress, inflammation and genotoxicity, leading to conflicting results [4]. Besides these endpoints, original effects of TiO_2-NP have also been described, e.g. impairment of cellular adhesion as well as autophagy [5-7]. Contrary to ultrafine particles, epidemiology failed to demonstrate a direct link between exposure to TiO_2-NPs and cancer. Large-scale –omics techniques, particularly proteomics, have been used in order to identify new pathways and endpoints for TiO_2-NP toxicity. These studies report that acute exposure to TiO_2-NPs induces a marginal cellular response [8] still it impacts cytoskeleton organization, cell metabolism, mitochondrial activity and induces a global stress response [9-12].

Most of the toxicology studies related to TiO_2-NPs have been conducted on cell lines exposed to very high concentrations of NPs and for very short times [4]. The cellular response to chronic exposure to low concentrations of TiO_2-NPs has only been approached very recently in a couple of articles. Briefly, long-term exposure to TiO_2-NPs alters cell cycle progression [13-15] and genome segregation during mitosis due to interference with mitotic spindle assembly and centrosome maturation [13]. It causes reactive oxygen species accumulation in exposed cells [15] as well as chromosomal instability [13] and cell transformation [13, 16].

In this context, the present study aimed at investigating proteome perturbations in A549 cells exposed for 2 months to a low or a high TiO_2-NP concentration, i.e. 2.5 µg/mL and 50 µg/mL, respectively. For cell exposure we used NM105 TiO_2-NPs from the nanoparticle library at Joint Research Center of the European Commission (JRC, Ispra, Italy), i.e. AEROXIDE® P25 TiO_2-NPs from Evonik. The rationale for using epithelial alveolar cells in this study is that, due to their physicochemical properties, NPs are prone to deposit in the alveolar region of the lung [2, 17]. We used 2D-gel proteomics to achieve this goal, because this technique investigates changes in protein abundances on a large scale, thereby providing a wider and untargeted view of the cellular functions impacted by biological stimuli of interest [18] while keeping the analysis at the protein level and not only at the peptide level. To the best of our knowledge, proteomics have never been used to assess cell response to a chronic exposure to TiO_2-NPs.

Materials and methods

Chemicals and reagents

Unless otherwise indicated, all chemicals and reagents were purchased from Sigma-Aldrich and were >99% pure.

Nanoparticles dispersion and characterization

TiO_2-NPs (AEROXIDE® P25, Evonik, Germany; NM105 as referenced in JRC, European Commission) were dispersed in ultrapure sterile water, to the concentration of 10 mg/mL, by applying high energy sonication at 4°C for 30 min (1s on/1s off), as described previously [19], using a probe sonicator equipped with a 3-mm microtip. The energy delivered by our sonicator was measured, amplitude of 28% corresponds to 16.7 W [20]. The physico-chemical properties of these TiO_2-NPs have already been described in our previous articles [19, 21]. Briefly, their crystalline structure is mixed anatase/rutile (86%/14%) [21], their primary diameter is 25±7 nm and their specific surface area is 46±1 m²/g [19]. Upon dispersion in water they form a stable suspension with average diameter (in number) of 44±25 nm and polydispersity index (PdI) 0.146±0.009 (data not shown). Suspensions in ultrapure water were stored in the darkness at room temperature. Just before cell exposure they were diluted in cell culture medium containing 10% FBS after vigorous vortexing. The average hydrodynamic diameter then reached 342±15 nm (in number) and PdI increased to 0.236±0.048, indicating that NPs agglomerated (data not shown).

Cell culture

A549 human lung carcinoma cells were purchased from ATCC (Manassas, VA, USA, reference CCL-185). Cells were subcultured in DMEM containing 4.5 g/L glucose (Life Technologies, Carlsbad, CA, USA) supplemented with 2 mM/L glutamine, penicillin/streptomycin (50 IU/mL and 50 mg/ml respectively, Life Technologies) and 10% vol./vol. FBS (Life Technologies). They were maintained at 37°C in a 5% CO_2/air incubator.

Exposure to NPs

During 2 months, cells were passed twice a week in 58 cm² petri dishes in cell culture medium containing NPs, using the following protocol: they were rinsed with PBS, trypsinized and counted after trypan blue staining. 1.25×10^6 cells per condition were then seeded in a new 58 cm² petri dish, using one petri dish per condition i.e. one petri dish per TiO_2-NP exposure concentration (0, 1, 2.5, 5, 10 or 50 µg/mL TiO_2-NPs). Therefore cells were exposed twice a week to a fresh suspension of NPs. The 10 mg/mL NP stock suspension was the same during the whole exposure period.

Proteomics

Sample preparation, 2D gel analysis and mass spectrometry were performed as already described [22]. Only the specific methods are described here.

Sample preparation

Cells exposed for 2 months to 2.5 or 50 µg/mL TiO_2-NPs (10^7 cells per condition, with three

independent biological replicates per condition, i.e. per exposure concentration) as well as control cells (also 10^7 cells in triplicate, not exposed to TiO_2-NPs) were collected by scraping and washed three times with PBS. They were then washed with TSE buffer (Tris-HCl 10 mM pH 7.5, sucrose 0.25 M, EDTA 1 mM), and the volume of the cell pellet was estimated by resuspension of the pellet in a known volume of TSE buffer and measurement of the suspension volume. Then 4 volumes of lysis buffer (urea 8.75 M, thiourea 2.5 M, CHAPS 5% w/v, TCEP-HCl, 6.25 mM, spermine base 12.5 mM) were added. After 1 h of incubation at room temperature, nucleic acids were removed by ultracentrifugation (270,000 g at room temperature for 1 h), and protein concentration in the supernatant was measured using the Bradford assay. Carrier ampholytes (Pharmalytes pH 3-10) were added to a final concentration of 0.4% (w/v). Samples were stored at -20°C until proteomic analysis.

Isoelectric focusing

Homemade long 4-8 linear pH gradient gels [23] were cast according to published procedures [24]. This pH interval was chosen as a good compromise between resolution and scope. Four mm-wide strips were cut, and rehydrated overnight with the sample, diluted in a final volume of 0.6 ml of rehydration solution (7 M urea, 2 M thiourea, 4% CHAPS, 0.4% carrier ampholytes (Pharmalytes pH 3-10) and 100 mM dithiodiethanol [25, 26]. Strips were then placed in a Multiphor plate (GE Healthcare, Little Chalfont, UK), and isoelectric focusing (IEF) was carried out with the following electrical parameters: 100 V for 1 h, then 300 V for 3 h, then 1000 V for 1 h, then 3400 V up to 60-70 kVh. After IEF, the gels were equilibrated for 20 min in Tris 125 mM, HCl 100 mM, SDS 2.5%, glycerol 30% and urea 6 M [27]. They were then transferred on top of SDS gels and sealed in place with 1% agarose dissolved in Tris 125 mM, HCl 100 mM, SDS 0.4% and 0.005% (w/v) bromophenol blue.

SDS electrophoresis and protein detection

Ten percent gels (160x200x1.5 mm) were used for protein separation [28]. The lower electrode buffer was Tris 50 mM, glycine 200 mM, SDS 0.1%. The gels were run at 25 V for 1 h then 12.5 W per gel until the dye front has reached the bottom of the gel. Detection was carried out by fast silver staining [29].

Image analysis

Gel images were analyzed using Delta 2D software v 3.6 (Decodon, Greifswald, Germany). Three gels were prepared from 3 independent cultures for each experimental group. Spots that were never present above 100 ppm of the total spots were first filtered out. Then, significantly-varying spots were selected on the basis of their Student T-test p-value between the different groups. Spots with a p-value lower than 0.05 were selected.

Mass spectrometry

Spots selected for identification were excised from the gels and analyzed using a NanoLC-MS/MS performed by a nanoLC-QTOF-MS system (Synapt G1 from Waters) and a nanoLC-QTOF-MS system (TripleTOF 6600 from ABSciex). For protein identification, MS/MS data were interpreted using a local

Mascot server with MASCOT 2.4.0 algorithm (Matrix Science, London, UK) against UniProtKB/SwissProt (version 2012_08, 537,505 sequences, [30]). Research was carried out in all species. A maximum of 1 trypsin missed cleavage was allowed. Spectra from QTOF were searched with a mass tolerance of 15 ppm for MS and 0.05 Da for MS/MS data. Carbamidomethylation of cysteine residues and oxidation of methionine residues were specified as variable modifications. Protein identifications were validated with at least 2 peptides with Mascot ion score above 20 or with 1 peptide with Mascot ion score above 30 and 5 consecutive fragment ions in MS/MS spectrum.
The mass spectrometry proteomics data have been deposited to the ProteomeXchange Consortium [31] via the PRIDE partner repository with the dataset identifier PXD002662.

Enolase activity

To confirm our proteomics results, α-enolase activity was measured by monitoring the conversion of 2-phosphoglycerate (2-PGA) into phosphoenolpyruvate (PEP) [32] in extracts from cells exposed to 0, 2.5 or 50 µg/mL NPs. Cell extracts were prepared by lysing 1.5×10^7 cells for 20 min at 0°C in 500 µl of Hepes 20 mM (pH 7.5) containing $MgCl_2$ 2 mM, KCl 50 mM, EGTA 1 mM and SB 3-14 (3-tetradecyldimethylammonio propane 1-sulfonate) 0.15% w./v., followed by centrifugation at 15,000 g for 15 min. Protein concentration was measured using Bradford assay. 200 µg of protein extract (40 µl) was then mixed with 400 µl of reaction buffer composed of 50 mM Tris-HCl, 1.5 mM 2-PGA and 1.5 mM $MgCl_2$ (pH 7.4). The appearance of PEP was followed by continuously measuring the absorbance at 240 nm at 20±1°C, on a Cary 60 UV-Vis (Agilent Technologies, Santa Clara, CA, USA) spectrophotometer, using an absorption coefficient of 1400 M^{-1} cm^{-1}. One unit of enzyme was defined as the amount of enzyme that converted 1 µmol 2-PGA into PEP in 1 min at 20°C. For calibration we used enolase from Baker's yeast (Sigma-Aldrich, reference E6126-500 UN).

Proteasome function

In order to evaluate the influence of proteasome on NP biological response, we evaluated the impact of MG132, a proteasome inhibitor, on the viability of cells exposed to 0, 2.5 or 50 µg/mL NPs [33]. After 2 months of exposure to NPs, cells were seeded at sub-confluence in 96-well plates, at 45 000 cells per well (6 wells per condition). Sixteen hours after plating, they were rinsed in fresh medium then exposed for 6 h to 100 µL of 1, 10 or 50 nM of MG132 (Ready-made solution, Sigma-Aldrich reference M7449). Cell viability was determined using the 3-[4,5-dimethylthiazol-2-yl]-2,5-diphenyl tetrazolium bromide (MTT) assay as described previously [21].

Mitochondrial activity

We used rhodamine 123 to evaluate mitochondrial membrane potential, as a marker of mitochondrial activity [34]. After 2 months of cell exposure to 0, 1, 2.5, 5, 10, 50 µg/mL TiO_2-NPs, cells seeded in 12-well plates at 70 000 cells per well (3 wells per condition). After 16 h, they were rinsed with fresh medium, then exposed to 200 µL of 1 µM rhodamine 123 (Life Technologies) for 30 minutes. Cells were then washed in PBS and collected by scraping. Fluorescence intensity was measured with excitation at 480 nm and emission at 530 nm, using a Spectramax M2 spectrophotometer (Molecular

Devices, Workingham, UK) and normalized with respect to protein concentration. Data were normalized with respect to protein concentration, reflecting cell number, measured using Bradford assay.

Western-Blot analyses

To investigate DNA damage response pathway activation, we determined phosphorylation and acetylation of the tumor suppressor protein p53 in cells chronically exposed to 0, 1, 2.5, 5, 10 or 50 µg/mL TiO_2-NP. 25×10^7 cells were lysed in a CellLytic™ M solution (Sigma-Aldrich) to which was added protease inhibitors (Complete Mini protease inhibitor cocktail tablets, Roche, Bâle, Switzerland, one tablet for 10 mL CellLytic solution) and Halt Phosphatase Inhibitor Cocktail (Thermo Fisher Scientific, Waltham, MA USA, 100 µL for 10 mL lysing mix), then centrifuged at 20000 rcf for 10 min at 4°C. Supernatants were kept at -80°C. Samples (30 µg protein content) were loaded in TGX Stain-Free™ FastCast™ Acrylamide 12% gels (Biorad, Hercules, CA, USA) and migrated at 100 V for 2 h. Proteins were transferred to a nitrocellulose membrane using the Trans-Blot® Turbo™ Transfert System (Biorad). These membranes were then blocked in 5% non-fat milk prepared in TBS/Tween 0.5% for 1 h. They were then incubated for 1h30 at room temperature with primary antibodies diluted in 5% non-fat dry milk prepared in TBS/Tween 0.5%: anti-phospho-p53 (Rabbit polyclonal to p53, phospho S15, Abcam, Cambridge, UK, reference ab1431, dilution 1/500 vol./vol.), anti-acetylated-p53 (Rabbit monoclonal EPR358(2) to p53 acethyl K382, Abcam, Cambridge, UK, reference ab75754, dilution 1/100 vol./vol.) and anti-p53 antibodies (Mouse monoclonal anti-p53, clone DO-1, Sigma-Aldrich, dilution 1/1000 vol./vol.). After rinsing in TBS-Tween 0.5%, membranes were incubated for 1 h at room temperature with anti-mouse and anti-rabbit secondary antibodies diluted in TBS/Tween 0.5% (Amersham ECL anti-mouse IgG HRP-linked, whole antibody, reference NA931 and Amersham ECL anti-rabbit IgG HRP-linked, whole antibody, reference NA934, dilution 1/20000 vol./vol. for both of them). Images were acquired on a Chemidoc XRS+ (Biorad) and band intensities were quantified with ImageLab software (Biorad). Results were normalized with respect to total protein content.

We also used Western Blot to determinate autophagy in control cells and cells exposed to 2.5 et 50 µg/mL NPs, by the conversion of microtubule-associated protein 1A/1B-light chain 3 from its cytosolic form (LC3-I) to LC3-phosphatidylethanolamine conjugate (LC3-II). The protocol was identical to what is described above using anti-LC3 antibody as primary antibody (LC3A/B (D3U4C) XP Rabbit mAb #12741, Cell Signaling Technology, Danvers, MA, USA, dilution 1/1000 vol./vol.) and anti-rabbit IgG as secondary antibody (Amersham ECL anti-rabbit IgG HRP-linked, whole antibody, reference NA934, dilution 1/20000 vol./vol.).

Cell cycle assessment

We assessed cell cycle as a possible consequence of the DNA damage pathway activation. After exposure to 0, 1, 2.5, 5, 10, 50 µg/mL TiO_2-NP cells were collected (10^6 cells per condition) and rinsed in PBS containing 2 mM EDTA (PBS-EDTA). Cells were fixed in ice-cold 70% ethanol for 30 min then washed with PBS-EDTA. They were suspended in PBS-EDTA containing 25 µg/mL propidium iodide (Life Technologies) and 25 µg/mL RNAse A (Sigma-Aldrich). A minimum of 20000 events per

condition was measured by flow cytometry using a FacsCalibur analyzer (BD Biosciences, Franklin Lanes, NJ, USA) equipped with the CXP software (Beckman Coulter Inc., Pasadena, CA, USA). Cell cycle data were fit using Flowing Software 2.5.1 (http://www.flowingsoftware.com/).

Cell proliferation assay

Proliferation was monitored using the 5-bromo-2'-deoxyuridine (BrdU) incorporation assay (Roche) in cells exposed to 0, 1, 2.5, 5, 10, 50 µg/mL TiO_2-NP according to the manufacturer's instructions. Briefly, cells were seeded in 96-well plates. They were exposed to BrdU for 16 hours before being fixed with FixDenat solution from the assay kit. They were then incubated in the anti-BrdU-POD antibody for 15 min (provided in the assay kit), then in the substrate solution for 5 min. BrdU labelling was then inferred from absorbance at 370 nm, measured using a Spectramax M2 spectrophotometer at 370 nm (Molecular Device), and corrected with respect to the absorbance at 490 nm.

Electron microscopy

After exposure, cells were fixed with 2.5% glutaraldehyde, post-fixed with OsO4 and dehydrated in graded concentrations of ethanol then embedded in Epon. Ultra-thin sections were cut (80 nm), counterstained with uranyl acetate and observed with a JEOL 1200 EX transmission electron microscope (TEM) operated at 80 kV (Grenoble Institut des Neurosciences, France) [35].

Statistical analysis

Experiments were repeated at least 3 times (biological replicates). Statistical tests were run using the Statistica 8.0 software (Statsoft, Chicago, IL, USA). Non-parametric one-way analyses of variance on ranks approach (Kruskal-Wallis) were used. When significance was demonstrated ($p < 0.05$), paired comparisons were run using Mann-Whitney tests.

Results

Proteomic analyses

Quantitative analysis of the proteome was carried out on whole cell extracts prepared from control cells (i.e. not exposed to TiO_2-NPs) or cells exposed for 2 months to either 2.5 or 50 µg/ml NPs (Figure 1).

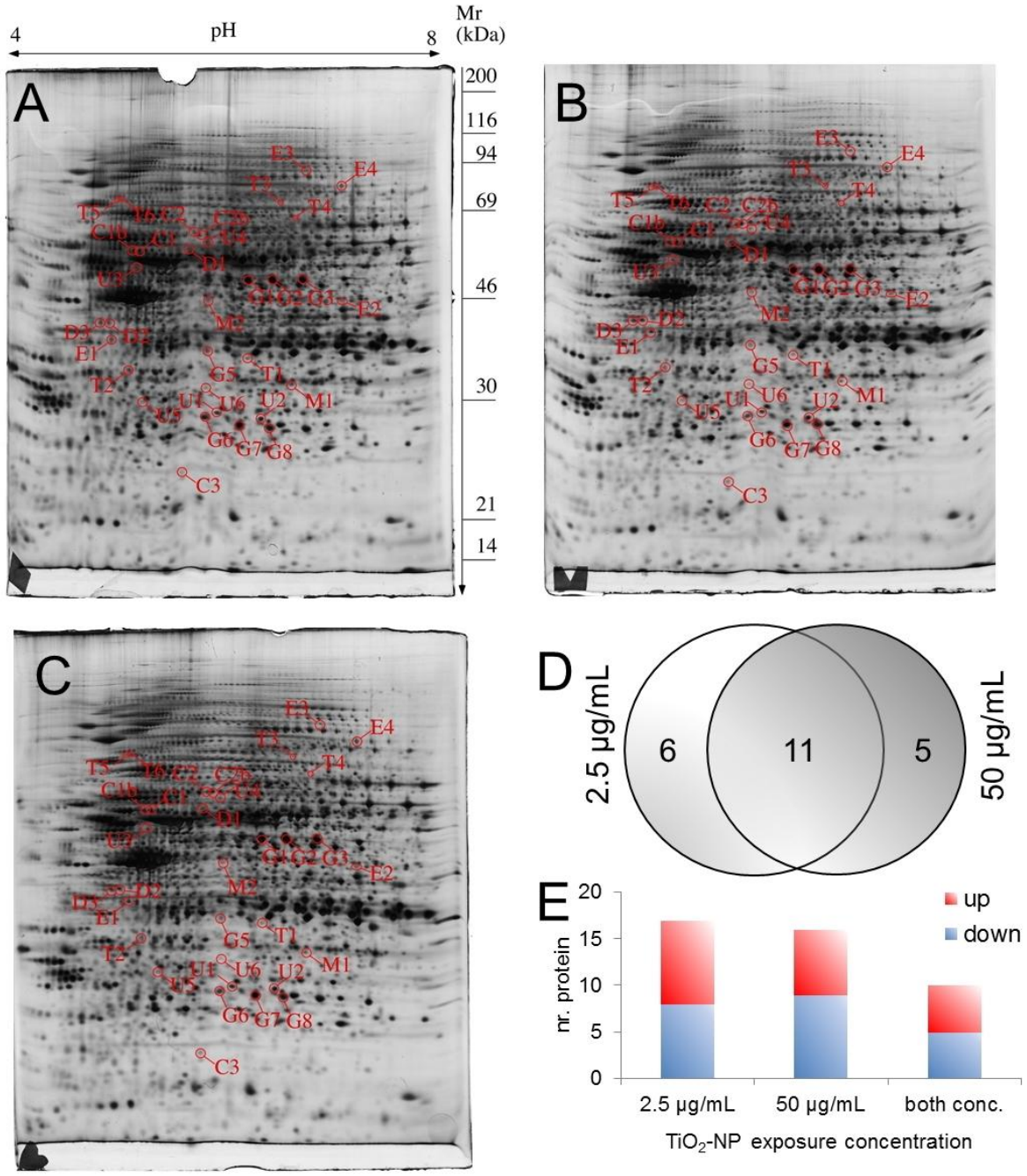

Figure 1: Proteomic analysis of total cell extracts by 2D-gel electrophoresis. Total cell extracts were separated by two-dimensional gel electrophoresis. The first dimension covered a 4-8 pH range and the second dimension a 15-200 kDa range. Proteins were detected by silver staining. Total cellular proteins (150 µg) were loaded on the first dimension gel. (A) gel obtained from control cells; (B) gel obtained from cells treated with 2.5 µg/mL TiO_2-NPs for 2 months; (C) gel obtained from cells treated with 50 µg/mL TiO_2-NPs for 2 months. Arrows point to spots that show statistically significant changes between the different samples. Spot numbering is accessible in Table 1. (D) Venn diagram representing the number of gene products with modulated content in cells exposed for 2 months to 2.5 or 50 µg/mL TiO_2-NPs, as well as gene products modulated in common at both exposure concentrations. (E) Number of gene products with content up- or down-regulated in each exposure condition.

Three biological replicates per condition prepared from independent cell cultures were analysed on 2D-gels (Figure 1A-C). We reproducibly detected 2310 spots on a pH 4-8 range, which was selected as a compromise between resolution (which decreases when the pH window increases) and scope (which increases when the pH window increases); since the literature reports that each protein corresponds to approximately 3 spots [36] these 2310 spots represent about 770 proteins species. The median coefficient of variation of spot intensity was 21%; it ranged between 13% and 25% depending on the sample i.e. within the range of typical 2D gel-based experiments [22, 37, 38].

Despite this rather limited proteome coverage, the abundance of at least one protein species from 22 gene products changed significantly in cells exposed to NPs, whatever the concentration, as compared to control cells. More precisely, the abundance of 17 and 16 gene products changed when comparing control cells to cells exposed to 2.5 µg/mL or 50 µg/mL TiO_2-NPs, respectively (Figure 1D). The abundance of 11 gene products was commonly modulated in cells exposed to both TiO_2-NP concentrations (Figure 1D). Increased content of 9, 7 and 5 proteins and decreased content of 8, 9 and 5 proteins was measured in cells exposed to 2.5 µg/mL TiO_2-NPs, 50 µg/mL TiO_2-NPs and both concentrations, respectively (Figure 1E). Except for one gene product (serine-threonine kinase receptor-associated protein), the fold-change was always higher in cells chronically exposed to 2.5 µg/mL as compared to cells exposed to 50 µg/mL TiO_2-NPs (Table 1).

We classified these proteins with respect to their function (Table 1). This classification made possible the identification of 6 main categories, corresponding to 6 main cellular functions that were impacted by TiO_2-NP exposure at the protein level. These categories are trafficking (5 proteins) glucose metabolism (3 proteins) gene expression (3 proteins) chaperones (2 proteins) mitochondrial activity (2 proteins) and DNA damage response (2 proteins). Protein abundances rather increased in the DNA damage response, chaperones and gene expression categories, while they rather decreased in the glucose metabolism and mitochondrial activity categories. In the trafficking category, the abundance of three proteins was reduced and the abundance of 2 proteins was increased. In addition to these 6 main categories, 5 gene products could not be classified in any category: peroxiredoxin-6 (spot U2) which is involved in oxidative stress response (note however that the most abundant spot of the same protein, spot U2, was not affected), 26-S proteasome non-ATP regulatory subunit 5, involved in proteasome activity; retinal dehydrogenase 1, implicated in the metabolism of vitamin A; chloride intracellular channel protein 4, which forms poorly selective ion channels in membranes and the NIT2 omega-amidase. These categories that we identified led us to investigate the functionality of their related cellular processes and structures.

Glucose metabolism perturbation

Our proteomics results showed decreased abundance of α-enolase (spots G1-G3 in Figure 1) and cytoplasmic malate dehydrogenase (spot G4) which are implicated in glucose metabolism. The intensity of the 3 α-enolase spots detected here, taken individually, was not modified significantly. Still their combined modulation implies that global α-enolase content is significantly decreased in cells exposed to the high concentration of TiO_2-NPs. Therefore to address the functional implication of this decreased protein content we monitored the enolase activity in extracts of cells exposed to 0, 2.5 and

50 µg/mL NPs. As indicated in Figure 2, our results also show that enolase activity was significantly reduced in cells exposed for 2 months to 50 µg/mL TiO_2-NPs. As we detected a rather small decrease in α-enolase amount in the proteomic screen, this does not mean necessarily that the activity is decreased. Indeed the diminution in amount can be compensated for by other mechanisms, including PTMs. Therefore to address the functional implication of this decreased protein content we monitored the enolase activity in extracts of cells exposed to 0, 2.5 and 50 µg/mL NPs. As indicated in Figure 2, our results also show that enolase activity was significantly reduced in cells exposed for 2 months to 50 µg/mL TiO_2-NPs. Enolase is a metalloenzyme that is present in all tissues capable of glycolysis. It is responsible for the conversion of 2-phosphoglucerate to phosphoenolpyruvate in the glycolysis metabolic pathway. The most abundant subunit in lung cells is the α subunit, the β and γ subunits being mostly present in muscle cells and neural tissues, respectively. In lung cells, decreased enolase activity is thus directly related to decreased α-enolase activity.

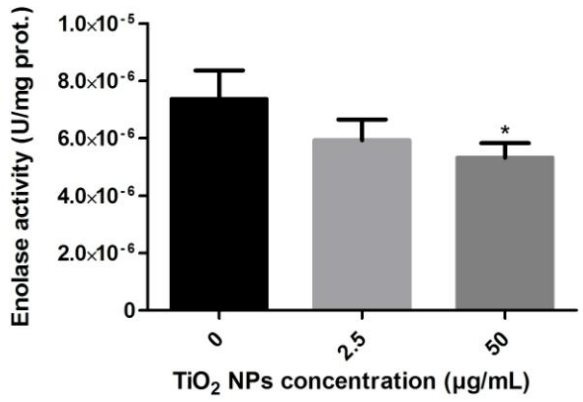

Figure 2: Enolase activity. Enolase activity was measured in extracts of cells exposed to 0, 2.5 or 50 µg/mL TiO_2-NPs, and normalized with respect to protein content. Results are presented as the mean of 4 points ± SEM. *: $p<0.05$ vs control.

The case of triose phosphate is more complex and illustrative of a situation commonly encountered in 2D gel-based proteomics. One of the spots (G5) is statistically different between control and TiO_2-exposed cells, while the other spots, which are more abundant (G6-G7) do not show any significant difference. However, the global trend for these metabolic proteins is decreased abundance, suggesting that exposure to NPs could impair this function.

Proteasome activity

Since our proteomic results showed decreased content of 26S proteasome non-ATPase regulatory subunit 5 (spot U3 in Figure 1) we suspected that the activity of proteasome could be impacted in A549 cells chronically exposed to TiO_2-NPs, as already described in dopaminergic neurons acutely exposed to TiO_2-NPs [39]. Therefore we monitored the ability of cells chronically exposed to 2.5 or 50 µg/mL of TiO_2-NPs to survive to a non-lethal concentration of MG132, a potent proteasome inhibitor [40]. The objective was to detect cytotoxicity that would be due to additive proteasome inhibition by

MG132 and by TiO_2-NPs, since excessive proteasome impairment is known to induce cell death [41]. On control cells, i.e. cells that were not exposed to TiO_2-NPs, MG132 was not cytotoxic (Figure 3). Conversely, significant mortality was observed in cells previously exposed to 2.5 µg/mL TiO_2-NPs for 2 months then post-exposed to 10 and 50 nM MG132. In cells chronically exposed to 50 µg/mL TiO_2-NPs the mortality rate was higher as compared to 2.5 µg/mL TiO_2-NPs; in this condition MG132 was cytotoxic at both 10 and 50 nM. This confirms that NPs exposure impaired proteasome activity, as anticipated from the proteomic results.

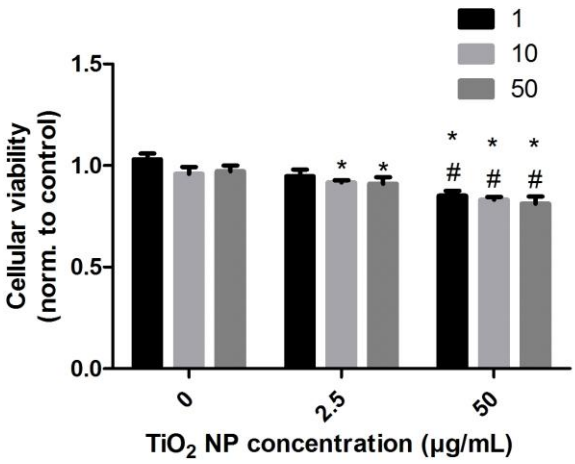

Figure 3: Proteasome role as a survival factor during NPs treatment. Following exposure to 0, 2.5 or 50 µg/mL TiO_2-NPs, cells were treated for 6 additional hours with 1, 10 or 50 nM of the proteasome inhibitor MG132. Cell viability was measured using the MTT assay. Results were normalized to control (without NPs or MG132) and are presented as the mean of 6 points ± SEM. *: $p<0.05$ vs control; #: $p<0,05$ vs 2.5 µg/mL NPs concentration at equivalent MG132 concentration.

Mitochondrial activity

Two proteins implicated in mitochondrial transport were less abundant in cells chronically-exposed to TiO_2-NPs, according to our proteomic results: beta-lactamase-like protein 2 (spot M1 in Figure 1) and mitochondrial import inner membrane translocase (spot M2). This suggests that mitochondrial activity may be impaired. We therefore measured mitochondrial membrane potential (ψ_m) which represents mitochondrial membrane polarization, a capital feature for ATP production. To do so, we measured the incorporation of rhodamine 123 in cells exposed to 0, 1, 2.5, 5, 10 or 50 µg/mL of TiO_2-NPs. We observed a concentration-dependent increase of its incorporation in cells exposed to 5, 10 and 50 µg/mL TiO_2-NPs (Figure 4A) which proves that long-term exposure to TiO_2-NPs induced mitochondrial membrane hyperpolarization. This increase confirms that NP exposure impairs global mitochondrial activity, as suggested by the proteomic results.

Classically, defective mitochondria are selectively removed from cells via mitophagy, which is a specific type of autophagy, in order to prevent cell degeneration [42]. The presence of mitochondria with altered functions in cells chronically exposed to TiO_2-NPs suggests that autophagy might be defective. To confirm this hypothesis we monitored the conversion of the cytoplasmic LC3-I into LC3-

phosphyatidylethanomaline (LC3-II) which is then recruited to the membranes of autophagosomes (Figure 4B). In addition we investigated the presence of autophasomoses by transmission electron microscopy (Figure (4C-D) in cells chronically exposed to 2.5 or 50 µg/mL TiO_2-NPs and control cells. We observed the presence of multiple autolysosomes containing agglomerates of nanoparticles (Figure 4B-C) together with multilamellar bodies. Moreover the conversion of LC3-II to LC3-I increased in cells exposed for 2 months to both 2.5 and 50 µg/mL TiO_2-NPs, suggesting that autophagy was induced.

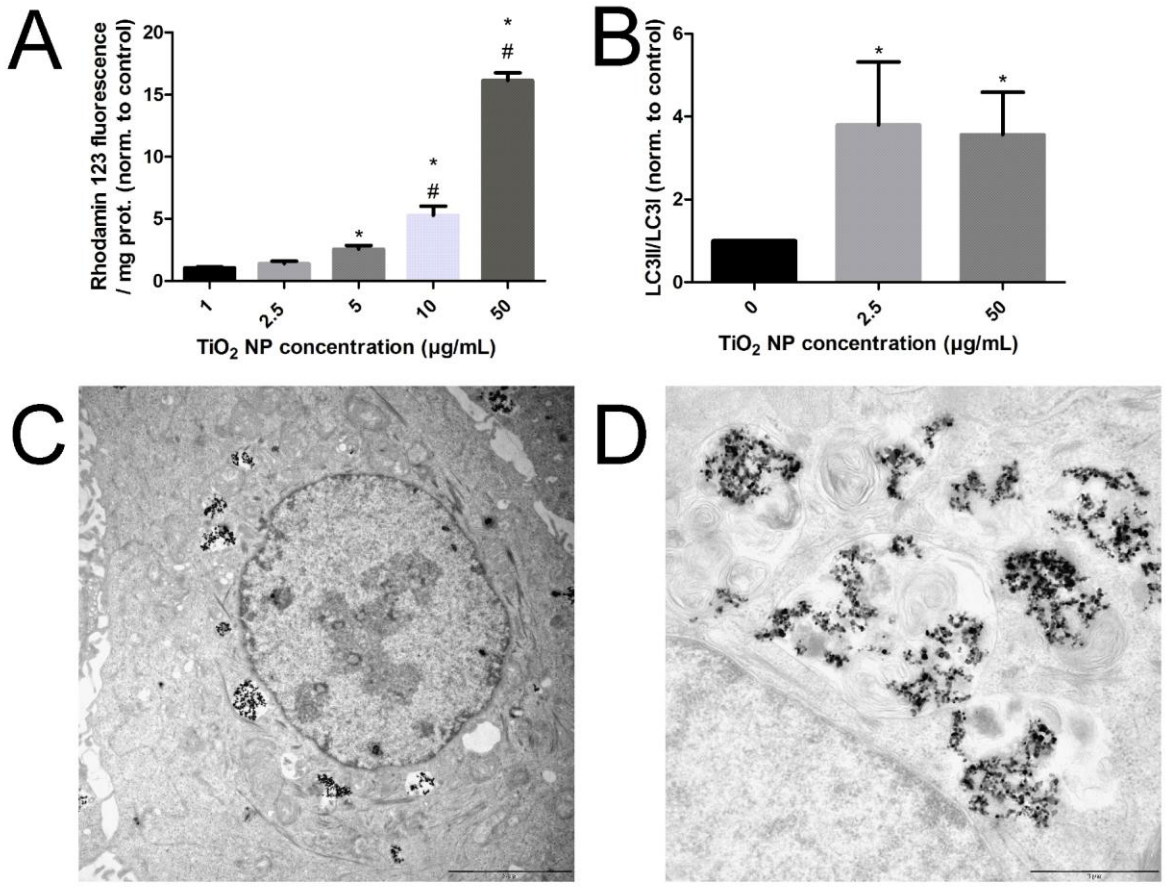

Figure 4: Mitochondrial activity impairment and induction of autophagy. (A) Mitochondrial membrane potential of cells exposed to TiO_2-NPs assessed using rhodamine 123. After NPs exposure, cells were exposed to 1 µM rhodamine 123 for 30 min. (B) LC3-I and LC3-II contents in A549 cells chronically exposed to 2.5 or 50 µg/mL TiO_2-NPs for 2 months. Results were normalized with respect to control data and are presented as the mean of 3 replicates ± SEM. *: $p<0.05$ vs control. (C-D) TEM images of A549 cells exposed to 50 µg/mL TiO_2-NPs for 2 months.

DNA damage response and its consequences

Our proteomic results displayed increased levels of 2 protein species of serine-threonine kinase receptor-associated protein (STRAP, spots D2-D3). STRAP has 2 roles: first, it stabilizes the tumour-suppressor p53 coactivators, p300 and JMY, so that they activate p53 [43]; second it acetylates p53

activating its inductive activity on DNA transcription [43]. Therefore, increased STRAP abundance could lead to p53 acetylation. As p53 acetylation is mediated by its phosphorylation [44], we monitored both p53 phosphorylation and acetylation by Western Blot after a 2 months exposure to 0, 1, 2.5, 5, 10 or 50 µg/mL TiO_2-NPs (Figure 5A). We observed significant increase in both post-translational modifications for all concentrations, except p53 phosphorylation at 1 µg/mL NPs. We therefore demonstrated the activation of the p53 signalling pathway in cells chronically exposed to TiO_2-NPs, confirming the effect that we anticipated from increased levels of STRAP.

Acetylation of p53 can lead to p21 activation, which in turn induces cell cycle arrest in G1 phase [45]. In addition another DNA damage-signalling protein highlighted by the proteomic results is protein phosphatase 5 (PP5, spot D1) which is also implicated in cell cycle regulation [46]. Taken together, these results suggest that NPs exposure could impact cell cycle. To confirm this hypothesis we monitored the cell cycle in cells exposed to 0, 1, 2.5, 5, 10 or 50 µg/mL TiO_2-NPs (Figure 5B). The proportion of cells in the G1 phase was moderately but significantly higher when cells had been chronically exposed to 50 µg/mL TiO_2-NPs, as compared to control cells. This increase was correlated with a decreased proportion of cells in the S phase after 2 months of exposure to 10 and 50 µg/mL NPs. This proves that cells encountered a moderate but significant slowdown of cell cycle progression following a concentration-dependent trend, confirming our hypothesis. We then investigated if this cell cycle slowing down had physiological consequences on cell proliferation (Figure 5C). We observed a concentration-dependent decrease of the cell proliferation rate in cells exposed 2.5, 5, 10 or 50 µg/mL TiO_2-NPs, confirming the physiological consequences of cell cycle modification caused by chronic exposure to TiO_2-NPs.

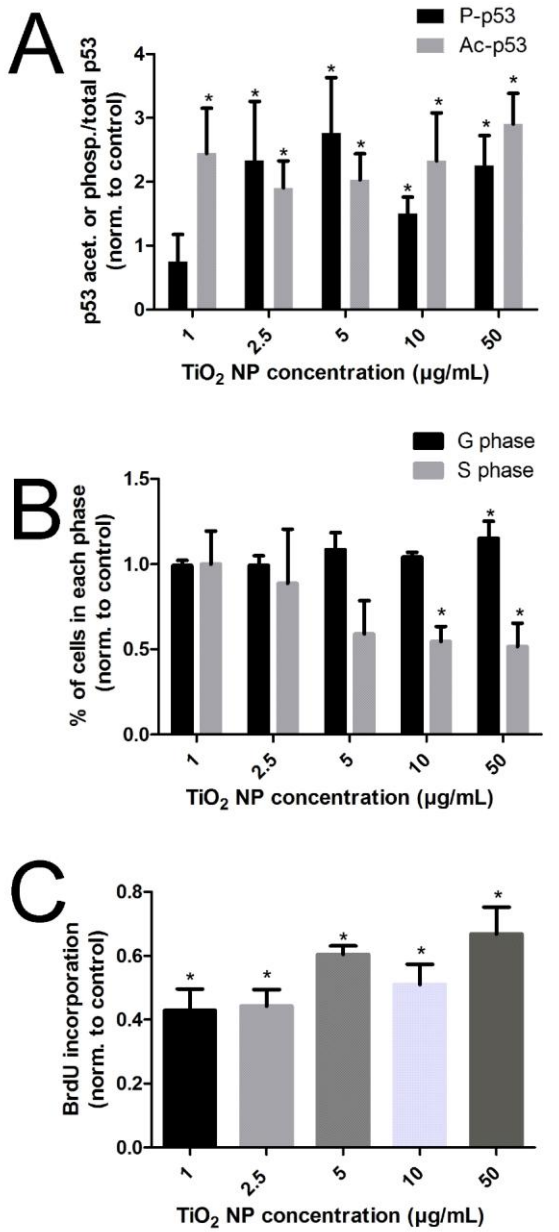

Figure 5: Induction of a DNA damage response. Post-translational modifications of p53 were assessed by Western Blot after exposure TiO_2-NPs. (A) Phosphorylation and acetylation data were reported to total p53 content, and normalized with respect to protein quantification using Stain-Free™ technology and to extracts of control cells. Results are presented as the mean of 3 points ± SEM. *: $p<0.05$ vs control. (B) Cell cycle analysis, showing percentage cells in the G1 phase and in the S phase compared to total cell number. Data were reported to the control. Results are presented as mean of 4 points ± SEM. *: $p<0.05$ vs control. (C) Cell proliferation after exposure to TiO_2-NPs, monitored by the BrdU incorporation assay. Results were reported to control data and are presented as the mean of 4 points ± SEM. *: $p<0.05$ vs control.

Discussion

This article describes the effects of long-term exposure of A549 cells to 2.5 and 50 µg/mL TiO_2-NPs, two concentrations which can be considered as a low and a high exposure concentration. Cell

response was assessed using 2D-gel proteomics analyses coupled to functional validation which, to enrich their strength, were for some of them also carried out in cells exposed for 2 months to 1, 5 and 10 µg/mL TiO_2-NPs.

We report significant modulation of abundance of only 22 protein species. In this respect, we observed several different cases when proteins were represented by several spots on the 2D gels. In the case of enolase, all the three spots decreased each in a weakly significant way, but the congruence of all variations became much more significant on a statistical point of view. We also observed cases where one modified (altered pI) spot was statistically significantly modulated, but the most abundant, basic spot(s) was(were) unchanged (dynein, triosephosphate isomerase, FKBP4, peroxiredoxin 6). Lastly, we also observed cases where all detected spots were significantly changed in the same direction (STRAP). This shows the complexity of the regulations phenomena that can be detected at the protein species level.

Compared to these 22 protein species, most proteomic studies related to the impact of acute exposure to TiO_2-NPs report a more intense cellular response, this discrepancy can easily be explained by the different exposure protocols, i.e. acute vs. chronic exposure and exposure medium containing vs. lacking FBS [9-12]. Moreover, this is certainly explained by the different cell models used in these different studies. Indeed, none of them were carried out on A549 cells. The different responses of different cell lines, but also of cell lines as compared to primary cells, have been largely reported. For instance a recent article shows that, among lung cell models, A549 and BEAS-2B respond differently and also respond differently from normal human primary bronchial epithelial cells (NHBE) [47]. A549 is from alveolar origin while BEAS-2B and NHBE originate from bronchial tubes. Moreover A549 originate from a lung carcinoma while BEAS-2B is a normal cell line transformed by SV40 and NHBE are non-immortalized, normal cells. Moreover A549 cells carry a number of mutations (for details see the COSMIC database, http://cancer.sanger.ac.uk/cosmic). All these differences can explain their different response."

We show that the cellular response to chronic exposure to both concentrations of TiO_2-NPs mostly consists in common elements. Indeed the content of 11 proteins, related to 6 functional categories, is modulated in both exposure conditions. The content of 6 and 5 proteins, related to the same 6 functional categories, is modulated in cells exposed to 2.5 µg/mL TiO_2-NPs only or 50 µg/mL TiO_2-NPs only, respectively. Interestingly, the modulation follows the same trend at both concentrations, i.e. when protein content was increased in cells exposed to 2.5 µg/mL TiO_2-NPs it was generally also increased in cells exposed to 50 µg/mL and reversely. Still the modulation is more intense in cells exposed to 2.5 µg/mL TiO_2-NPs than in cells exposed to 50 µg/mL TiO_2-NPs. Chronicity and low TiO_2-NP concentration would thus induce a stronger molecular response of exposed cells, possibly because at this low concentration cells maintain their optimal capacity to adapt to this external repeated stress. This underlines the necessity to use realistic, low-concentrations of NPs when assessing the biological impact of NPs, particularly when probing the level of modulation of a specific pathway. This also highlights that exposure to a high concentration of NPs makes possible the identification of cellular structures and functions that are also affected at more realistic, low concentrations. Consequently, in our exposure conditions, high exposure concentration is predictive of

the cellular pathways that are affected in the more realistic, low concentration exposure condition. Our functional experiments also show that the same functions are affected in cells exposed at high and low concentrations of NPs.

We report here that chronic exposure to TiO_2-NPs causes activation of the DNA damage response pathway, via p53 activation, leading to impairment of cell cycle progression and cell proliferation. In this context, an important point to keep in mind is that A549 cells present a p53 wild type phenotype (http://www.lgcstandards-atcc.org/~/media/2B3C84F951E24E668C78EB70809C7613.ashx) even though they arise from a carcinoma. Thus, investigating the function of p53 with this model is appropriate. P53 is a central player in the DNA damage response. Its activation can be directly caused by the DNA damage that we and others previously reported in cells exposed to TiO_2-NPs either acutely [4, 21, 48] or chronically [13] and which is characterized by oxidative lesions and DNA strand breaks, including double-strand breaks that may result from the duplication of cells with replication fork blockade [48]. It may also be linked to the impaired glucose metabolism that our proteomics results reveal; indeed p53 is also activated upon cell starvation and metabolic stress [49]. Its activation can lead to cell cycle arrest, senescence or apoptosis, depending on the mode of activation and DNA damage duration [50]. In our experiments, activation of p53 is correlated with increased content of STRAP in cells chronically exposed to TiO_2-NPs, which suggest that p53 is activated via the ATM pathway [51]. STRAP is a cofactor of p53 which stabilizes it by antagonizing Mdm2 and by stabilizing JMY and p300, two other cofactors of p53. Moreover STRAP activity enhances p53 acetylation, which activates p53-mediated transcription. By increasing STRAP intracellular content, chronic exposure to TiO_2-NPs thus induces DNA damage response, which may lead to the transcription of DNA repair genes. Finally phosphorylation of p53 [52] cell proliferation impairment [53] and activation of the ATM pathway [54] have already been observed in targeted, non-proteomic studies, evaluating the impact of acute exposure to NPs on other cell models. We thus show here that activation of p53 is also a significant determinant of the impact of long-term exposure to TiO_2-NPs of A549 lung cells.

We also report here decreased contents of two mitochondrial enzymes, together with hyperpolarization of mitochondrial membrane which signs mitochondrial activity impairment. Hyperpolarization of mitochondria also occurs in cells exposed to a variety of small molecules [55], to rapamycin [56], salinomycin [57] and glutamate [58]. It can be due to either increased proton pumping by increased activity of respiratory enzyme complexes, blockade of electron transfer, blockade of the use of protons by enzymes within the mitochondria or change in the mitochondrial pH, leading to membrane potential modifications. Mitochondrial damage is often correlated with the onset of autophagy [56, 57] which has largely been described as a mechanism of NP toxicity upon acute exposure of mammalian cells, *in vitro* [59] and particularly in cells acutely exposed to TiO_2-NPs [60]. It may be an attempt to eliminate damaged organelles, particularly the damaged mitochondria. Indeed damaged mitochondria are classically eliminated via mitophagy, which is a specialized type of autophagy [42]. It may also be a way to sequester and discard NPs accumulated in the cytoplasm, which is supported by our TEM observations showing cells containing numerous autolysosomes filled

with NPs. Mitochondrial damage is related to oxidative stress, since mitochondria and the respiration are the main source of endogenous reactive oxygen species (ROS) in mammalian cells. Perturbation of mitochondrial activity may lead to the accumulation of ROS that was previously reported after acute [4, 21, 48] or chronic [13, 15] exposure to TiO_2-NPs, which correlated well with the onset of oxidative damage of DNA [21, 48]. Still, here we report decreased abundance of only one protein species related to oxidative stress response, peroxiredoxin-6. However, neither the more abundant spot of the same protein nor the levels of the other peroxiredoxins were modified upon TiO_2 treatment suggesting a low level of oxidative stress, i.e. efficient scavenging of the ROS produced in cells upon long-term exposure to TiO_2-NPs.

Broadly speaking, decreased glucose metabolism, along with decreased proteasome and mitochondrial activity suggests global cell impairment. Increased content of molecular chaperones confirms the presence of a context of cellular stress [61] which might be linked with the activation of the DNA damage response pathway. All these modifications might lead to the decrease of cell proliferation that we report here. However the absence of overt cytotoxicity, associated with the increased content of proteins involved in gene expression also suggest that cells are fighting this stress and might recover over time. Moreover, in addition to being a general stress response, increased chaperone contents might be linked either with increased gene expression or with the compensation of decreased proteasome activity. Indeed a decrease of proteasomal activity will result in higher levels of unfolded proteins to be handled by chaperones, as previously described in other contexts of cellular stress [62] and among them in neuron cells acutely exposed to TiO_2-NPs [39]. It again suggests that the cellular response to acute TiO_2-NP exposure reflects well the cellular response to a more realistic long-term exposure.

Lastly, we report modulations of abundances of proteins involved in cell trafficking. We observed a decreased content of calponin-2, a protein that is involved in cell motility and cytokinesis [63] and a decreased abundance of annexin A4, which plays a role in exocytosis [64]. These two proteins are involved in exchange mechanisms with the environment of the cell; the results reported here thus suggest that cells chronically-exposed to TiO_2-NPs reduce their communication with the extracellular compartment due to the intracellular stress [65]. On the other hand, we observe decrased content of vesicle-fusing ATPase, kinesin light chain 2 and increased content of the acidic, activated form of dynein [66]. These proteins are involved in intracellular transport [66, 67]. This suggests that cells chronically exposed to TiO_2-NPs tend to limit their interactions with their environment and to modulate intracellular transport. It can be interpreted as a defence mechanism, comparable to the increased abundance of chaperones proteins.

The categories of proteins reported here as being impacted by long-term exposure to TiO_2-NPs, particularly mitochondrial activity, trafficking, glucose metabolism have also been identified by proteomics in cells acutely exposed to TiO_2-NPs [9-12]. In spite of these similarities, the DNA damage response activation that we observe here was either absent or very attenuated in these other studies.

The only study mentioning DNA damage is the one by Tilton *et al.* [12]. Instead, these papers displayed increased contents of proteins involved in the apoptotic pathway [9-12] which is a feature that we do not observe. Apoptosis often occurs in cells encountering non-repaired DNA damage, and one could speculate that cells chronically exposed to TiO_2-NPs might to some extent efficiently repair DNA damage therefore preventing apoptosis, contrary to cells acutely exposed to higher, toxic concentrations of TiO_2-NPs. This observation is in line with the hypothesis that cells exposed to a low, sub-toxic concentration of NPs are able to efficiently face this stress that may eventually trigger an adaptive response.

Lastly, new mechanisms emerge from this study when comparing the pathways identified here by proteomics analysis to those already described and resulting from targeted experiments [13-16]. The principal mechanisms described to date were over-production (or not) of ROS [13, 15, 16], genotoxicity or no DNA damage [13, 16], tumorigenesis and cell transformation [13, 16], as well as impairment of cell cycle progression [13-15] by inhibition of mitotic progression [13]. We report here that cell cycle progression impairment is certainly linked to the DNA damage response which is activated via production of STRAP and phosphorylation/acetylation of p53; and that it ultimately leads to reduced cell proliferation and DNA repair. We also show mitochondrial impairment, which might cause or be caused by the oxidative stress that is very classically reported in cells exposed to TiO_2-NPs and which might itself cause the initiation of autophagy and/or mitophagy. In this global scene we also show altered proteasome activity and glucose metabolism, activation of the production of chaperones as well as reduced trafficking towards the extracellular compartment, signing a defence mechanism. This study thus made possible the identification of new modes of action of TiO_2-NPs upon chronic exposure.

Conclusions

This study gives new insights in TiO_2-NP toxicity upon long-term exposure. At rather small, non-cytotoxic concentrations, several biological pathways are altered including mitochondrial activity or glucose metabolism. In addition the activation of DNA damage responses and its biological consequences in terms of p53 activation, cell cycle modification and cell proliferation strongly suggest a cellular stress, even at the lowest concentration of NPs. However, the absence of apoptosis-related protein induction and cytotoxicity, along with the increased contents of proteins and chaperone-related proteins, suggests that cells are fighting against this stress. Finally we show that the use of high exposure concentrations is predictive of the cellular response to lower, more realistic exposure concentrations. Still we observed that the lowest concentrations and longest exposure periods induced the more intense cellular response. Taken together, these data suggest that long-term exposure to low concentrations of TiO_2-NPs may induce cell adaptation but not overt mortality.

Acknowledgements

This work was funded by CEA through the Nanoscience and Toxicology research programs, and via the European Commission's 7th Framework Programme project NanoMILE (Contract No. NMP4-LA-2013-310451). It is a contribution to the Labex Serenade (n° ANR-11-LABX-0064) funded by the "Investissements d'Avenir" French Government program of the French National Research Agency (ANR) through the A*MIDEX project (n° ANR-11-IDEX-0001-02). We also thank the Proteomexchange/PRIDE team for providing public access to our data [67]

Conflict of interest

The authors declare no conflict of interest.

Table 1. Proteins showing different contents in control cells vs. cells exposed to TiO_2-NPs, identified in the proteomic screen[a]

Spot ID	Protein name	Accession number[a]	Molecular weight (Da)	Nr. unique peptide	Sequence coverage	2.5/Ctrl (Fold/T-test)	50/Ctrl (Fold/T-test)
DNA damage response							
D1	Serine/threonine-protein phosphatase 5	P53041	56880	12	31,10%	1.644/0.02	1.235/0.21
D2	*Serine-threonine kinase receptor-associated protein*	Q9Y3F4	38439	18	67,10%	1.503/0.043	1.637/0.004
D3	*Serine-threonine kinase receptor-associated protein*	Q9Y3F4	38439	20	69,10%	1.322/0.115	1.536/0.014
Chaperones							
C1	Peptidyl-prolyl cis-trans isomerase FKBP4	Q02790	51806	24	55,30%	1.544/0.034	1.185/0.047
C2	Peptidyl-prolyl cis-trans isomerase FKBP4	Q02790	51806	23	62,70%	1.544/0.082	1.054/0.50
C3	T-complex protein 1 subunit gamma	P49368	60535	22	42,40%	2.245/0.058	1.881/0.018
Mitochondrial activity							
M1	*Beta-lactamase-like protein 2*	Q53H82	32807	13	54,90%	0.584/0.048	0.805/0.29
M2	*Mitochondrial import inner membrane translocase subunit TIM44*	O43615	51357	10	24,80%	0.713/0.02	0.537/0.002
Gene expression							
E1	Eukaryotic translation initiation factor 2 subunit 1	P05198	36113	22	64,40%	1.937/0.025	1.73/0.046
E2	Multifunctional protein ADE2	P22234	47080	15	41,60%	0.964/0.91	1.891/0.032
E3	Putative pre-mRNA-splicing factor ATP-dependent RNA helicase DHX15	O43143	91009	19	25,20%	1.692/0.027	1.195/0.244
Trafficking							
T1	Calponin-2	Q99439	33698	7	31,40%	0.478/0.048	0.796/0.152

T2	Annexin A4	P09525	35884	10	35,40%	0.501/0.031	0.768/0.021
T3	Vesicle-fusing ATPase	P46459	82597	15	21,90%	2.263/0.024	1.524/0.15
T4	Kinesin light chain 2	Q9H0B6	68936	10	17,40%	0.342/0.03	0.552/0.063
T5	Cytoplasmic dynein 1 intermediate chain 2	Q13409	68377	9	17,60%	1.619/0.034	1.446/0.068
T6	Cytoplasmic dynein 1 intermediate chain 2	Q13409	68377	9	19,80%	1.200/0.62	1.065/0.87
Glucose metabolism							
G1	*Alpha-enolase*	P06733	47170	34	73%	1.12/0.58	0.81/0.16
G2	*Alpha-enolase*	P06733	47170	33	75,00%	1.11/0.52	0.94/0.61
G3	*Alpha-enolase*	P06733	47170	37	77%	1.14/0.53	0.9/0.63
G4	Malate dehydrogenase cytoplasmic	P40925	36427	4	14,10%	0.513/0.026	0.798/0.11
G5	Triosephosphate isomerase	P60174	30791	15	21,90%	0.592/0.01	0.759/0.017
G6	Triosephosphate isomerase	P60174	30791	24	71,00%	0.86/0.17	1.0/1
G7	Triosephosphate isomerase	P60174	30791	25	71%	0.94/0.7	1.07/0.65
Miscellaneous							
U1	Peroxiredoxin-6	P30041	25036	11	48,20%	0.612/0.009	0.941/0.566
U2	Peroxiredoxin-6	P30041	25036	16	56%	1.095/0.19	0.93/0.38
U3	*26S proteasome non-ATPase regulatory subunit 5*	Q16401	56197	17	44,20%	0.885/0.67	0.529/0.04
U4	Retinal dehydrogenase 1	P00352	54863	16	40,50%	0.681/0.11	0.574/0.017
U5	Chloride intracellular channel protein 4	Q9Y696	28774	14	67,20%	0.931/0.84	1.574/0.02
U6	Omega-amidase NIT2	Q9NQR4	30609	10	45,30%	0.756/0.82	0.499/0.045

[a]The accession numbers are those of the SwissProt Database. The proteins directly or indirectly validated are in italics in the table.

References

[1] Robichaud CO, Uyar AE, Darby MR, Zucker LG, Wiesner MR. Estimates of Upper Bounds and Trends in Nano-TiO2 Production As a Basis for Exposure Assessment. Environmental Science & Technology. 2009;43:4227-33.

[2] Oberdorster G, Oberdorster E, Oberdorster J. Nanotoxicology: an emerging discipline evolving from studies of ultrafine particles. Environ Health Perspect. 2005;113:823-39.

[3] Loomis D, Grosse Y, Lauby-Secretan B, El Ghissassi F, Bouvard V, Benbrahim-Tallaa L, et al. The carcinogenicity of outdoor air pollution. Lancet Oncology. 2013;14:1262-3.

[4] Shi H, Magaye R, Castranova V, Zhao J. Titanium dioxide nanoparticles: a review of current toxicological data. Particle and Fibre Toxicology. 2013;10.

[5] Bernier MC, Besse M, Vayssade M, Morandat S, El Kirat K. Titanium dioxide nanoparticles disturb the fibronectin-mediated adhesion and spreading of pre-osteoblastic cells. Langmuir. 2012;28:13660-7.

[6] Zarogiannis SG, Filippidis AS, Fernandez S, Jurkuvenaite A, Ambalavanan N, Stanishevsky A, et al. Nano-TiO(2) particles impair adhesion of airway epithelial cells to fibronectin. Respir Physiol Neurobiol. 2013;185:454-60.

[7] Zhao Y, Howe JL, Yu Z, Leong DT, Chu JJ, Loo JS, et al. Exposure to titanium dioxide nanoparticles induces autophagy in primary human keratinocytes. Small. 2013;9:387-92.

[8] Triboulet S, Aude-Garcia C, Armand L, Collin-Faure V, Chevallet M, Diemer H, et al. Comparative proteomic analysis of the molecular responses of mouse macrophages to titanium dioxide and copper oxide nanoparticles unravels some toxic mechanisms for copper oxide nanoparticles in macrophages. PLoS One. 2015;10:2015.

[9] Ge Y, Bruno M, Wallace K, Winnik W, Prasad RY. Proteome profiling reveals potential toxicity and detoxification pathways following exposure of BEAS-2B cells to engineered nanoparticle titanium dioxide. Proteomics. 2011;11:2406-22.

[10] Gao Y, Gopee NV, Howard PC, Yu LR. Proteomic analysis of early response lymph node proteins in mice treated with titanium dioxide nanoparticles. J Proteomics. 2011;74:2745-59.

[11] Sund J, Palomaki J, Ahonen N, Savolainen K, Alenius H, Puustinen A. Phagocytosis of nano-sized titanium dioxide triggers changes in protein acetylation. J Proteomics. 2014;108:469-83.

[12] Tilton SC, Karin NJ, Tolic A, Xie Y, Lai X, Hamilton RF, Jr., et al. Three human cell types respond to multi-walled carbon nanotubes and titanium dioxide nanobelts with cell-specific transcriptomic and proteomic expression patterns. Nanotoxicology. 2014;8:533-48.

[13] Huang S, Chueh PJ, Lin Y-W, Shih T-S, Chuang S-M. Disturbed mitotic progression and genome segregation are involved in cell transformation mediated by nano-TiO2 long-term exposure. Toxicology and Applied Pharmacology. 2009;241:182-94.

[14] Kocbek P, Teskac K, Kreft ME, Kristl J. Toxicological Aspects of Long-Term Treatment of Keratinocytes with ZnO and TiO2 Nanoparticles. Small. 2010;6:1908-17.
[15] Wang S, Hunter LA, Arslan Z, Wilkerson MG, Wickliffe JK. Chronic Exposure to Nanosized, Anatase Titanium Dioxide Is Not Cyto- or Genotoxic to Chinese Hamster Ovary Cells. Environmental and Molecular Mutagenesis. 2011;52:614-22.
[16] Vales G, Rubio L, Marcos R. Long-term exposures to low doses of titanium dioxide nanoparticles induce cell transformation, but not genotoxic damage in BEAS-2B cells. Nanotoxicology. 2014;19:1-11.
[17] Human respiratory tract model for radiological protection. A report of a Task Group of the International Commission on Radiological Protection. Ann ICRP. 1994;24:1-482.
[18] Rabilloud T, Lescuyer P. Proteomics in mechanistic toxicology: History, concepts, achievements, caveats, and potential. Proteomics. 2015;15:1051-74.
[19] Simon-Deckers A, Gouget B, Mayne-L'Hermite M, Herlin-Boime N, Reynaud C, Carriere M. In vitro investigation of oxide nanoparticle and carbon nanotube toxicity and intracellular accumulation in A549 human pneumocytes. Toxicology. 2008;253:137-46.
[20] Brun E, Barreau F, Veronesi G, Fayard B, Sorieul S, Chaneac C, et al. Titanium dioxide nanoparticle impact and translocation through ex vivo, in vivo and in vitro gut epithelia. Part Fibre Toxicol. 2014;11:1743-8977.
[21] Jugan M-L, Barillet S, Simon-Deckers A, Herlin-Boime N, Sauvaigo S, Douki T, et al. Titanium dioxide nanoparticles exhibit genotoxicity and impair DNA repair activity in A549 cells. Nanotoxicology. 2012;6:501-13.
[22] Triboulet S, Aude-Garcia C, Armand L, Gerdil A, Diemer H, Proamer F, et al. Analysis of cellular responses of macrophages to zinc ions and zinc oxide nanoparticles: a combined targeted and proteomic approach. Nanoscale. 2014;6:6102-14.
[23] Gianazza E, Celentano F, Magenes S, Ettori C, Righetti PG. Formulations for immobilized pH gradients including pH extremes. Electrophoresis. 1989;10:806-8.
[24] Rabilloud T, Valette C, Lawrence JJ. Sample application by in-gel rehydration improves the resolution of two-dimensional electrophoresis with immobilized pH gradients in the first dimension. Electrophoresis. 1994;15:1552-8.
[25] Rabilloud T, Adessi C, Giraudel A, Lunardi J. Improvement of the solubilization of proteins in two-dimensional electrophoresis with immobilized pH gradients. Electrophoresis. 1997;18:307-16.
[26] Luche S, Diemer H, Tastet C, Chevallet M, Van Dorsselaer A, Leize-Wagner E, et al. About thiol derivatization and resolution of basic proteins in two-dimensional electrophoresis. Proteomics. 2004;4:551-61.
[27] Gorg A, Postel W, Gunther S, Weser J, Strahler JR, Hanash SM, et al. Approach to stationary two-dimensional pattern: influence of focusing time and immobiline/carrier ampholytes concentrations. Electrophoresis. 1988;9:37-46.
[28] Tastet C, Lescuyer P, Diemer H, Luche S, van Dorsselaer A, Rabilloud T. A versatile electrophoresis system for the analysis of high- and low-molecular-weight proteins. Electrophoresis. 2003;24:1787-94.

[29] Chevallet M, Luche S, Rabilloud T. Silver staining of proteins in polyacrylamide gels. Nat Protoc. 2006;1:1852-8.
[30] Consortium U. UniProt: a hub for protein information. Nucleic Acids Res. 2015;43:27.
[31] Vizcaino JA, Deutsch EW, Wang R, Csordas A, Reisinger F, Rios D, et al. ProteomeXchange provides globally coordinated proteomics data submission and dissemination: Nat Biotechnol. 2014 Mar;32(3):223-6. doi: 10.1038/nbt.2839.; 2014.
[32] Pal-Bhowmick I, Sadagopan K, Vora HK, Sehgal A, Sharma S, Jarori GK. Cloning, over-expression, purification and characterization of Plasmodium falciparum enolase. Eur J Biochem. 2004;271:4845-54.
[33] Unnithan AS, Choi HJ, Titler AM, Posimo JM, Leak RK. Rescue from a two hit, high-throughput model of neurodegeneration with N-acetyl cysteine. Neurochem Int. 2012;61:356-68.
[34] Triboulet S, Aude-Garcia C, Carriere M, Diemer H, Proamer F, Habert A, et al. Molecular responses of mouse macrophages to copper and copper oxide nanoparticles inferred from proteomic analyses. Mol Cell Proteomics. 2013;12:3108-22.
[35] Dorier M, Brun E, Veronesi G, Barreau F, Pernet-Gallay K, Desvergne C, et al. Impact of anatase and rutile titanium dioxide nanoparticles on uptake carriers and efflux pumps in Caco-2 gut epithelial cells. Nanoscale. 2015;7:7352-60.
[36] Hoogland C, Mostaguir K, Sanchez JC, Hochstrasser DF, Appel RD. SWISS-2DPAGE, ten years later. Proteomics. 2004;4:2352-6.
[37] Winkler DF, McGeer PL. Protein labeling and biotinylation of peptides during spot synthesis using biotin p-nitrophenyl ester (biotin-ONp). Proteomics. 2008;8:961-7.
[38] Jehmlich N, Dinh KH, Gesell-Salazar M, Hammer E, Steil L, Dhople VM, et al. Quantitative analysis of the intra- and inter-subject variability of the whole salivary proteome. J Periodontal Res. 2013;48:392-403.
[39] Wu J, Xie H. Effects of titanium dioxide nanoparticles on alpha-synuclein aggregation and the ubiquitin-proteasome system in dopaminergic neurons. Artif Cells Nanomed Biotechnol. 2014;11:1-5.
[40] Lee DH, Goldberg AL. Proteasome inhibitors: valuable new tools for cell biologists. Trends Cell Biol. 1998;8:397-403.
[41] Han YH, Park WH. Proteasome inhibitor MG132 reduces growth of As4.1 juxtaglomerular cells via caspase-independent apoptosis. Arch Toxicol. 2010;84:689-98.
[42] Yoshii SR, Mizushima N. Autophagy machinery in the context of mammalian mitophagy: Biochim Biophys Acta. 2015 Jan 26. pii: S0167-4889(15)00022-1. doi: 10.1016/j.bbamcr.2015.01.013.; 2015.
[43] Demonacos C, Krstic-Demonacos M, Smith L, Xu D, O'Connor DP, Jansson M, et al. A new effector pathway links ATM kinase with the DNA damage response. Nat Cell Biol. 2004;6:968-76.
[44] Sakaguchi K, Herrera JE, Saito S, Miki T, Bustin M, Vassilev A, et al. DNA damage activates p53 through a phosphorylation-acetylation cascade. Genes Dev. 1998;12:2831-41.
[45] Macleod KF, Sherry N, Hannon G, Beach D, Tokino T, Kinzler K, et al. p53-dependent and independent expression of p21 during cell growth, differentiation, and DNA damage. Genes Dev. 1995;9:935-44.
[46] Hinds TD, Jr., Sanchez ER. Protein phosphatase 5. Int J Biochem Cell Biol. 2008;40:2358-62.

[47] Ekstrand-Hammarstrom B, Akfur CM, Andersson PO, Lejon C, Osterlund L, Bucht A. Human primary bronchial epithelial cells respond differently to titanium dioxide nanoparticles than the lung epithelial cell lines A549 and BEAS-2B. Nanotoxicology. 2012;6:623-34.
[48] Kansara K, Patel P, Shah D, Shukla RK, Singh S, Kumar A, et al. TiO2 nanoparticles induce DNA double strand breaks and cell cycle arrest in human alveolar cells. Environ Mol Mutagen. 2015;56:204-17.
[49] Khan D, Katoch A, Das A, Sharathchandra A, Lal R, Roy P, et al. Reversible induction of translational isoforms of p53 in glucose deprivation. Cell Death Differ. 2015;2015:220.
[50] Speidel D. The role of DNA damage responses in p53 biology. Arch Toxicol. 2015;89:501-17.
[51] Shiloh Y, Ziv Y. The ATM protein kinase: regulating the cellular response to genotoxic stress, and more. Nat Rev Mol Cell Biol. 2013;14:197-210.
[52] Belade E, Chrusciel S, Armand L, Simon-Deckers A, Bussy C, Caramelle P, et al. The role of p53 in lung macrophages following exposure to a panel of manufactured nanomaterials. Arch Toxicol. 2014;2014:7.
[53] Marquez-Ramirez SG, Delgado-Buenrostro NL, Chirino YI, Iglesias GG, Lopez-Marure R. Titanium dioxide nanoparticles inhibit proliferation and induce morphological changes and apoptosis in glial cells. Toxicology. 2012;302:146-56.
[54] Prasad RY, Chastain PD, Nikolaishvili-Feinberg N, Smeester L, Kaufmann WK, Fry RC. Titanium dioxide nanoparticles activate the ATM-Chk2 DNA damage response in human dermal fibroblasts. Nanotoxicology. 2013;7:1111-9.
[55] Montague CR, Fitzmaurice A, Hover BM, Salazar NA, Fey JP. Screen for small molecules increasing the mitochondrial membrane potential. J Biomol Screen. 2014;19:387-98.
[56] Paglin S, Lee NY, Nakar C, Fitzgerald M, Plotkin J, Deuel B, et al. Rapamycin-sensitive pathway regulates mitochondrial membrane potential, autophagy, and survival in irradiated MCF-7 cells. Cancer Res. 2005;65:11061-70.
[57] Jangamreddy JR, Ghavami S, Grabarek J, Kratz G, Wiechec E, Fredriksson BA, et al. Salinomycin induces activation of autophagy, mitophagy and affects mitochondrial polarity: differences between primary and cancer cells. Biochim Biophys Acta. 2013;2013:2057-69.
[58] Kumari S, Mehta SL, Li PA. Glutamate induces mitochondrial dynamic imbalance and autophagy activation: preventive effects of selenium. PLoS One. 2012;7:19.
[59] Stern ST, Adiseshaiah PP, Crist RM. Autophagy and lysosomal dysfunction as emerging mechanisms of nanomaterial toxicity. Part Fibre Toxicol. 2012;9:1743-8977.
[60] Tang Y, Wang F, Jin C, Liang H, Zhong X, Yang Y. Mitochondrial injury induced by nanosized titanium dioxide in A549 cells and rats. Environ Toxicol Pharmacol. 2013;36:66-72.
[61] Kalmar B, Greensmith L. Induction of heat shock proteins for protection against oxidative stress. Adv Drug Deliv Rev. 2009;61:310-8.
[62] Esser C, Alberti S, Hohfeld J. Cooperation of molecular chaperones with the ubiquitin/proteasome system. Biochim Biophys Acta. 2004;29:1-3.
[63] Wu KC, Jin JP. Calponin in non-muscle cells. Cell Biochem Biophys. 2008;52:139-48.

[64] Willshaw A, Grant K, Yan J, Rockliffe N, Ambavarapu S, Burdyga G, et al. Identification of a novel protein complex containing annexin A4, rabphilin and synaptotagmin. FEBS Lett. 2004;559:13-21.
[65] Keating DJ. Mitochondrial dysfunction, oxidative stress, regulation of exocytosis and their relevance to neurodegenerative diseases. J Neurochem. 2008;104:298-305.
[66] Vaughan PS, Leszyk JD, Vaughan KT. Cytoplasmic dynein intermediate chain phosphorylation regulates binding to dynactin. J Biol Chem. 2001;276:26171-9.
[67] Hirokawa N, Noda Y, Tanaka Y, Niwa S. Kinesin superfamily motor proteins and intracellular transport. Nat Rev Mol Cell Biol. 2009;10:682-96.